PERGAMON

International Journal of Multiphase Flow 28 (2002) 347–361

International Journal of Multiphase Flow

www.elsevier.com/locate/ijmulflow

Subcooled boiling of surfactant solutions

G. Hetsroni *, M. Gurevich, A. Mosyak, R. Rozenblit, L.P. Yarin

Department of Mechanical Engineering, Technion – Israel Institute of Technology, Haifa 32000, Israel

Received 4 October 2000; received in revised form 2 September 2001

Abstract

Boiling heat transfer from horizontal stainless steel tubes, submerged in subcooled surfactant solutions of various concentrations, was studied experimentally. The kinetic of boiling (bubble nucleation, growth and departure) was investigated by high-speed video recording in combination with Infrared Thermography. The specific features of boiling of surfactant solutions were revealed. It was found that the subcooled nucleate boiling of surfactant could not be described by a single curve, in contrast to water. A boiling hysteresis was found for degraded solutions. This phenomenon may be related to formation of a surfactant monolayer, which results in damping of an interfacial motion. © 2002 Elsevier Science Ltd. All rights reserved.

Keywords: Pool boiling; Subcooled boiling; Surfactant; Heat flux; Degraded solution

1. Introduction

Boiling heat transfer is of great interest in such traditional problem as the power generation as well as in cooling of microelectronic systems, desalination of seawater, etc.

The study of saturated pool boiling of a surfactant solution shows a significant enhancement of the heat transfer (Morgan et al., 1949; Sephton, 1974; Wasekar and Manglik, 1999; Hetsroni et al., 2001) in contrast to heat transfer in turbulent pipe flow with surfactants (e.g. Hetsroni et al., 1997). It was shown by Sephton (1974) that addition of small amounts of surfactants to seawater could substantially enhance the boiling desalination process. Gannet and Williams (1971) concluded that surface tension was not relevant in explaining the enhancement effect, and reported

---

* Corresponding author. Tel. +972-48-292-058; fax: +972-48-343-362.
E-mail address: hestroni@tx.technion.ac.il (G. Hetsroni).

PII: S0301-9322(01)00062-3

that viscosity could be a successful correlating parameter. On the other hand, Yang and Maa (1983) showed that the surface tension of the surfactant solution had significant influence on the heat transfer coefficient at boiling of a dilute sodium lauryl benzene sulfonate and sodium lauryl sulfate solution.

Pool boiling experiments were carried out by Tzan and Yang (1990) for a wide range of surfactant concentrations and heat fluxes. The results verify again that a small amount of surface-active additive makes the nucleate boiling heat transfer coefficient considerably higher. It was also found that there is an optimum additive concentration for the highest heat flux. Further increase in the concentration of the additive lowers the boiling heat transfer coefficient. Wu et al. (1995) reported experimental data on the effect of surfactants on nucleate boiling heat transfer in water with nine different additives. Anionic, cationic, and nonionic surfactants were studied at concentration up to 400 ppm. The enhancement of heat transfer was related to the depression of the static surface tension. Boiling heat transfer coefficients were measured by Ammerman and You (1996) for an electrically heated platinum wire immersed in saturated water, and in water mixed with three different concentrations of sodium dodecyl sulfate (an anionic surfactant). Their results showed that addition of an anionic surfactant to water caused an increase in the convection component and a corresponding reduction in the latent heat component of the heat flux in the fully developed boiling region. The comprehensive reviews on the heat transfer in nucleate pool boiling of aqueous surfactants and polymeric solutions have been published by Kandlikar and Alves (1999) and Wasekar and Manglik (1999). It was shown that surfactant additives at low concentrations could enhance the nucleate boiling heat transfer significantly.

An application of surfactants for the heat transfer enhancement is limited by the temperature of the water solution, which leads to some degradation of the surfactants. This issue is discussed in the present paper.

The objective of the present investigation is to study the heat transfer and bubble dynamics in the solution at various concentrations of the surfactant. The effect of fluid bulk temperature on subcooled boiling as well as the behavior of degraded solutions are also considered.

We used the cationic surfactant Habon G of molecular weight 500 (trade name Hoe S4089, Hoechst A.G.). The surfactant is hexadecyldimethyl hydroxyethyl ammonium and the counterion is 3-hydroxy 2-naphtoate. The surfactant molecules form large rod-shaped micelles. It was shown by Zakin et al. (1996) that although the microstructure of Habon G was mechanically degraded under high shear conditions, it recovered quickly – no matter how many times it was broken up by shear.

2. Physical properties of surfactant solutions

The dependence of the shear viscosity, surface tension and thermal conductivity of fresh Habon G solution on the temperature has been described by Hetsroni et al. (2001). It was shown that the surface tension decreases with both increases in concentration and in temperature. The temperature effect on the surface tension is much stronger at temperatures near the saturation temperature. It was shown also that the thermal conductivity was close to that for pure water within the uncertainty of the measurements. However, the effect of the temperature on the kinematic viscosity and surface tension in fresh and degraded surfactant solutions is different.

2.1. Fresh solutions

The measurements of physical properties were carried out over a wide range of temperatures and for various concentrations. All solutions used were prepared by dissolving the powdered surfactant in deionized water, with gentle stirring, over a period of several days. Concentrations, *C*, investigated here were 130–1060 ppm (parts per million weight).

The effect of temperature on the kinematic viscosity of the fresh surfactant solution for various Habon G concentrations is depicted in Fig. 1(a). An increase in surfactant concentration is accompanied by an increase in the kinematic viscosity. An increase in the solution temperature, *T*, leads to monotonous decrease in the kinematic viscosity. The dependence of the Prandtl number on the temperature is shown in Fig. 1(b), for water and different concentrations of Habon G solutions. The Prandtl number is defined as $Pr = \nu/\alpha$, where $\alpha = k/\rho c_p$ is the thermal diffusivity (ν is the kinematic viscosity, κ is the thermal conductivity, ρ is the density and c_p is specific heat at

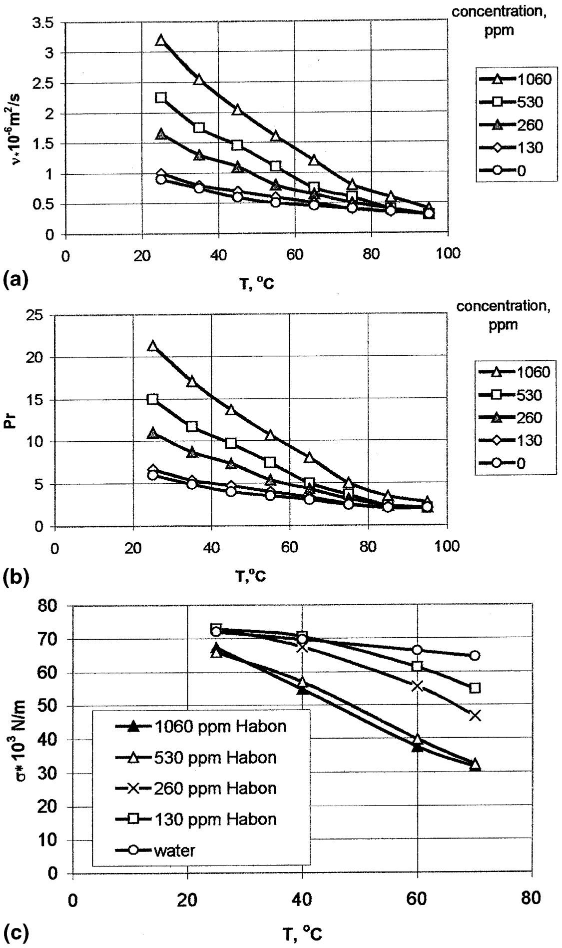

Fig. 1. Physical properties of fresh solutions: (a) kinematic viscosity; (b) Prandtl number; (c) surface tension.

constant pressure). In all the cases an increase in the liquid temperature leads to a decrease in the Prandtl number. The surface tension was measured in the temperature range of 25–70 °C. The data were obtained by using a SensaDyne PC500-LV Surface Tensiometer System, which measured surface tension within the body of a test fluid by blowing a bubble of gas through two probes of different diameters inside the body.

The kinematic viscosity was measured by a Cannon–Fenske capillary viscometer. The thermal conductivity was measured by using the thermal comparative method (Hetsroni et al., 2001). The apparatus was of a steady-state type. The density and heat capacity were taken to be those of the solvent, since the concentration did not exceed 1000 ppm.

Fig. 1(c) shows the surface tension as a function of temperature of various concentrations of Habon G. As seen in this figure, the surface tension decreases with an increase in both the concentration and the temperature. The temperature effect on the surface tension is much stronger at temperatures near the saturation temperature, whereas the opposite trend is observed for the viscosity. All physical properties were measured with standard deviation of 2%.

2.2. Degraded solutions

The data on the kinematic viscosity of degraded surfactant solutions corresponding to various concentrations of Habon G are presented in Fig. 2(a). The dependence of $\nu(T)$ for degraded and fresh solutions is significantly different. Such difference manifests itself more for high concentration of Habon G: at $C \geqslant 550$ ppm the curves $\nu(T)$ are not monotonous. In this case, the viscosity of the surfactant solution increases with temperature within the range ($20 < T < 60$ °C) and decreases at temperatures $T > 60$ °C. The maximum viscosity of the degraded surfactant solution

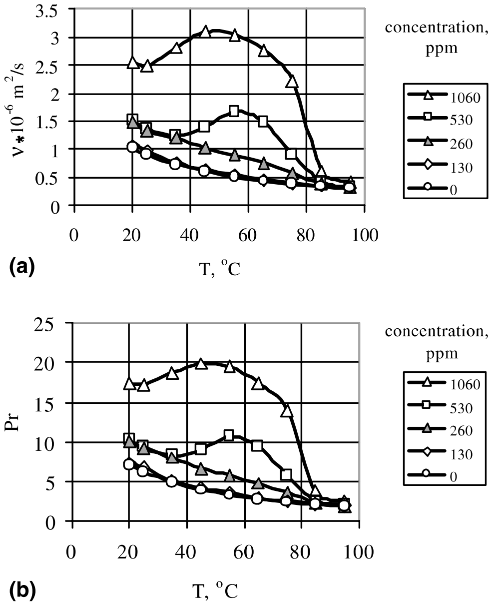

Fig. 2. Physical properties of degraded solutions: (a) kinematic viscosity; (b) Prandtl number.

corresponds to a temperature about 55–60 °C. Fig. 2(b) shows the dependence of the Prandtl number on the temperature.

The data on the surface tension of degraded solutions do not differ from that for fresh one within the uncertainty limits.

3. Experimental

3.1. Apparatus

Two sets of apparatus were used. The experimental facility for the study of subcooled boiling from a horizontal stainless steel tube is shown in Fig. 3. It consists of a rectangular vessel (140 mm long, 90 mm wide and 100 mm deep) with transparent walls, a thermostat to regulate the bulk fluid temperature, the heated tube, two copper bars and electric contacts. The heated part of the tube ($d_{\mathrm{out}} = 1.5$ mm, $d_{\mathrm{in}} = 1.0$ mm) was 40 mm long. It was fixed in a horizontal position along the longitudinal centerline of the pool at a distance of 40 mm from the bottom. Electric current was supplied to the heated tube through copper bars from a DC power supply. A calibrated, Teflon coated, T-type thermocouple of diameter 0.3 mm was inserted inside the heated tube. The thermocouple could be adjusted exactly to any desired position in the heated tube. The temperature of the outer surface was calculated from the power dissipation per unit volume of the tube. The measurements showed that the temperature along the tube was uniform, within an accuracy of ±0.1 °C. The bulk temperature was maintained constant within ±0.2 °C by the thermostat and was measured by a T-type thermocouple with an accuracy ±0.1 °C.

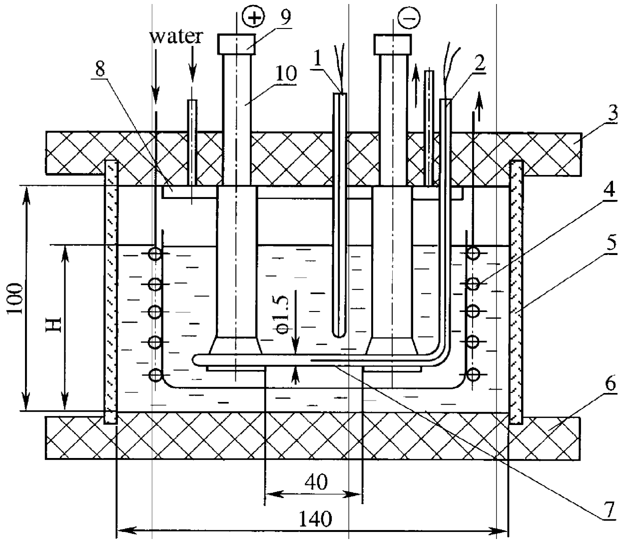

Fig. 3. Experimental setup. 1 – thermocouple for the fluid bulk temperature, 2 – thermocouple inside of the tubular heating element, 3 – upper plate, 4 – thermostat, 5 – glass wall, 6 – bottom, 7 – tubular heating element, 8 – condenser, 9 – electrical contact, 10 – copper bar.

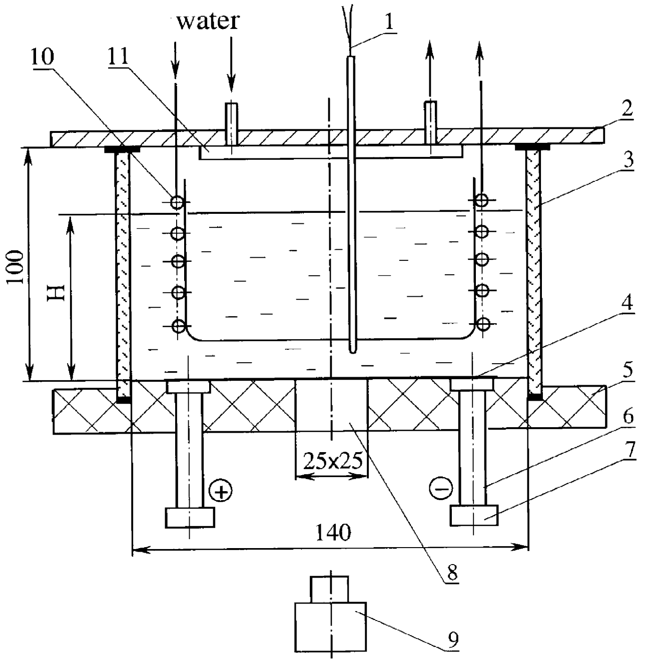

Fig. 4. Experimental facility used for study heat transfer from horizontal surface. 1 – thermocouple, 2 – upper plate, 3 – glass wall, 4 – heater made of stainless steel foil, 5 – lower plate, 6 – copper bar, 7 – electrical contact, 8 – window, 9 – IR-camera, 10 – cooler, 11 – condenser.

The second apparatus is depicted in Fig. 4. It was used to explore boiling heat transfer from a horizontal heated surface facing upward. Boiling occurred over a constantan foil of 0.05 mm thickness. The foil was heated by DC current and the heat flux on the wall could be regulated. An infrared image of the heater was recorded from below by an Infrared Radiometer.

3.2. Instrumentation

The growth of bubbles and the bubble motion near the heated surface were recorded by a high-speed video camera with recording rate up to 10 000 frames per second. The playback speed can be varied from a single frame to 250 frames per second. An IR radiometer was used in the investigation of the thermal pattern on the heater. The radiometer has a typical minimum detectable temperature difference of 0.1 K. The time response of these instruments is limited by the video system format (25 frames per second). The image has horizontal resolution of 256 pixels per line and 256 intensity levels. Since the foil is very thin, the temperature difference between the two sides of the foil does not exceed 0.2 K at a heat flux of 100 kW/m^2 (Hetsroni and Rozenblit, 1994). Therefore, the time-averaged temperature was almost the same on both sides of the foil. The surface temperature and the surfactant bulk temperature were measured with an accuracy of 0.1 K. Electrical power was determined by means of a digital wattmeter with an accuracy of ±0.5%. The bias contribution, *B*, and precision limit, *P* (95% confidence level), were calculated by means of following the equations (Kline and McClintock, 1953). The results are given in Table 1, where

Table 1
Uncertainty of the measurements

Item	Designation	Bias limit B (%)	Precision limit P (%)
Heat flux	q	1	2
Wall temperature	T_W	0.1	1
Bulk temperature	T_B	0.5	2
Saturation temperature	T_S	0.1	0.2
Temperature difference	$T_W - T_S$	3	6
Heat transfer coefficient	h	3	7

the bias limit is an estimate of the magnitude of the fixed constant error. The precision limit is an estimate of the lack of repeatability caused by random errors and insteadiness.

4. Results

4.1. Subcooled water boiling

This study was conducted to investigate a pool boiling phenomena at various levels of subcooling. For a subcooled liquid, the system bulk temperature T_B is maintained below than the saturation temperature T_S at a given system pressure. The difference between the saturation and system temperature is the degree of subcooling.

Tests were conducted in an open pool (atmospheric pressure) at three different water temperatures: $T_B = 40, 60, 70$ °C. In Fig. 5 the heat flux is plotted vs. wall superheat ($T_W - T_S$), where T_W is the temperature of the heated surface. Previous investigators (Johansen, 1991; Hong et al., 1997) have reported that this temperature difference allowed to present the boiling data for all levels of subcooling by a single boiling curve. It can be concluded from Fig. 5 that boiling data for

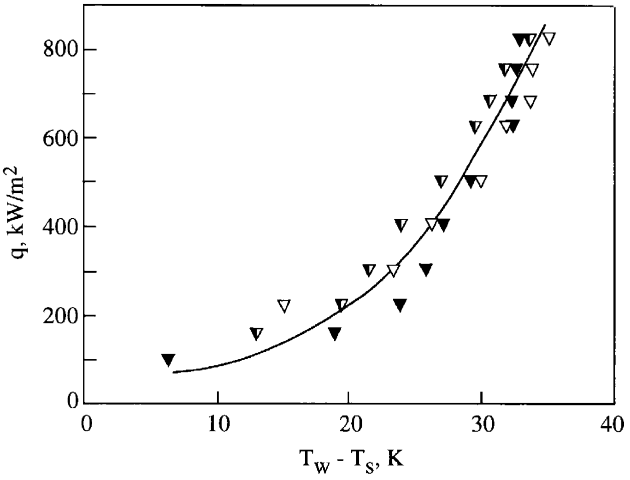

Fig. 5. Boiling curves for the subcooled water. Bulk temperatures T_B (°C): ∇ – 40, ⧨ – 60, ▼ – 70.

subcooling levels of 60, 40 and 30 K may be described by single curve with a standard deviation of 11%. This merging of data indicates that the boiling curve is insensitive to the subcooling level in the range of examined temperatures.

Carey (1992) reported that the boiling curve usually changes very little with an increase in the level of subcooling. Judd and Hwang (1976) observed independence of the wall temperature vs. level of subcooling in methylene chloride at boiling on a flat glass surface. Mudawar and Anderson (1989) discussed the effects of subcooling in pool boiling of FC-72 on vertically mounted flat heaters. There was no substantial difference in the boiling characteristic, during nucleate boiling for two different levels of subcooling 20 and 35 K. Our data agree well with results reported by previous investigators.

4.2. Boiling of subcooled fresh surfactant solutions

4.2.1. Flow visualization

In order to provide a description of the flow pattern under high heat fluxes, we studied pool boiling on the stainless steel tube of outer diameter 1.5 mm. Fig. 6(a) and (b) shows typical pictures for both water and the Habon G (550 ppm) solution boiling at heat flux $q = 700\ \mathrm{kW/m^2}$ and the bulk temperature $T_B = 60$ °C. The bubble dynamics for water depends on the heat flux and is similar to well-known data of boiling visualization. After the onset of nucleate boiling the regime of single bubbles occurs close to the heated wall (Fig. 6(a)). Fig. 6(b) shows boiling of 530 ppm Habon G solution under the same conditions. The Habon G additive reduces significantly the tendency of coalescence between vapor bubbles. The bubbles grow continuously and collapse

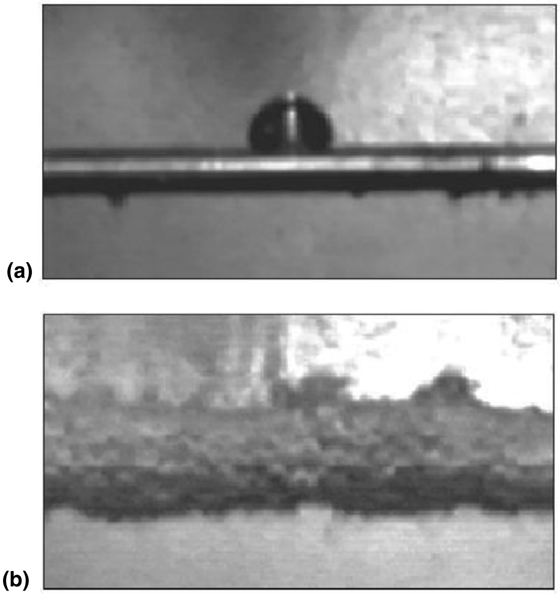

Fig. 6. Visualization of the subcooled boiling on the horizontal tube, Bulk temperature $T_B = 60$ °C, heat flux $q = 700\ \mathrm{kW/m^2}$: (a) water; (b) 530 ppm Habon G solution.

on the tube. The bubbles are smaller in size but much larger in number than in the case of pure water. They appear on the heated tube in a quite orderly manner.

4.2.2. Thermal pattern

The temperature distribution on the heated wall for degraded 530 ppm Habon G solution at the fluid bulk temperature $T_B = 40$ °C is shown in Fig. 7(a) and (b) at the heat fluxes $q = 90$ and 110 kW/m^2, respectively. The histogram of the thermal field at $q = 90$ kW/m^2 on the heated wall corresponds to natural convection. In this case boiling does not occur, because the maximum wall temperature $T_W = 100$ °C (Fig. 7(a)). At $q = 110$ kW/m^2 boiling takes place on the surface. The magnitude of the standard deviation of the surface temperature decreases compared to the case with natural convection. However, the variation of the wall temperature is more than 20 K. It is clear that the models for a bubble nucleation and growth that assume uniformity of the wall excess temperature cannot be realistic at such wide variation of the wall temperature.

4.2.3. Boiling curves

The experiments were performed in the range of heat flux 100–800 kW/m^2 at temperatures of the solutions $T_B = 40, 60, 70$ °C. The typical experimental conditions are given in Table 2. Data were taken for both increasing and decreasing heat fluxes. The bath temperature was adjusted to obtain the desired level of subcooling within the test vessel, during the time required for the experimental runs. The total mass of the liquid in the test facility remained constant, thus no fresh

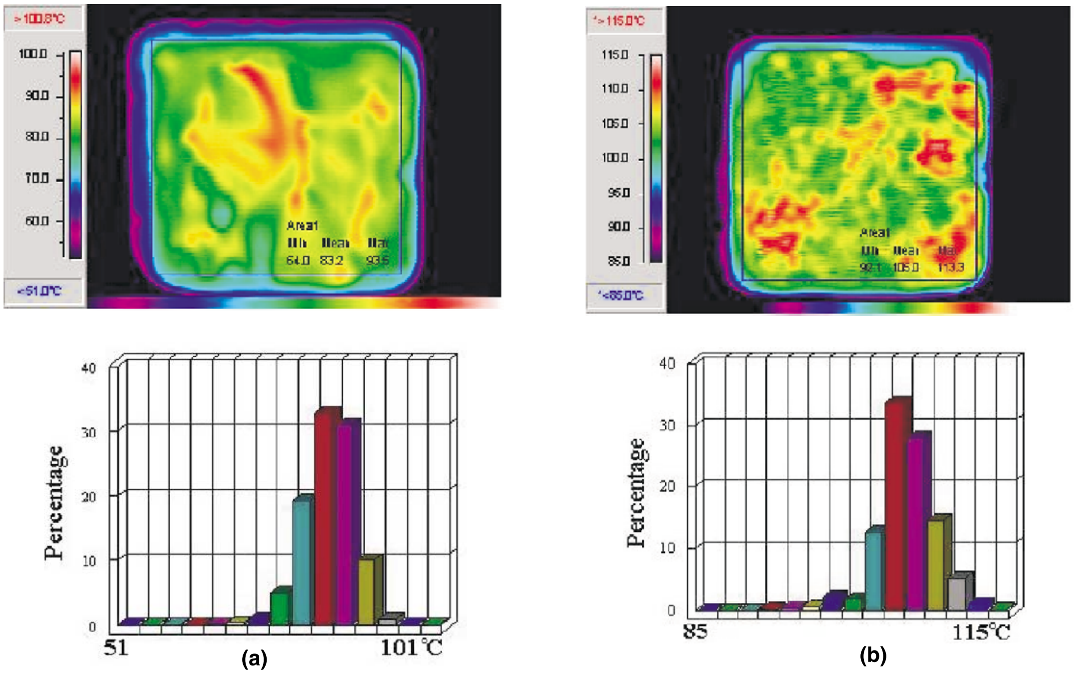

(a) (b)

Fig. 7. Thermal pattern and histograms for degraded 530 ppm Habon G solution. Bulk temperature $T_B = 40$ °C: (a) $q = 90$ kW/m^2 ; (b) $q = 110$ kW/m^2.

Table 2
Subcooled boiling of fresh Habon G solutions

Concentration C (ppm)	Bulk temperature T_B (°C)	Symbols	Heat flux q (kW/m^2)			
			220	400	620	820
			Wall temperature T_W (°C)			
130	40	◇	114.9	119.6	123.4	124.6
	60	⬘	114.9	120.3	123.7	124.7
	70	◆	114.8	119.7	123.0	123.7
260	40	□	114.0	117.9	120.5	121.6
	60	⬒	114.3	117.2	119.9	121.4
	70	■	113.4	116.8	119.7	121.3
530	40	△	111.0	114.5	117.2	119.9
	60	◭	111.6	114.2	117.4	120.7
	70	▲	111.4	114.4	117.5	120.8
1060	60	◓	109.2	112.8	115.3	116.6
	70	•	108.1	111.2	114.0	115.9

liquid was introduced to "top off" the system. Boiling curves for Habon G solutions in the subcooled states are shown in Fig. 8 (see also Table 3). The heat flux, q, is plotted against the wall superheat $T_W - T_S$ (the natural convection data are not shown). The subcooled nucleate boiling curve of water is also shown in this figure. Each point in Fig. 8 represents an average value obtained from the measurements. In these experiments we did not observe any signs of a hysteresis. This figure clearly demonstrates that the definition of heat flux vs. the wall superheat $(T_W - T_S)$ provides the description of all subcooled states by a common curve only for a surfactant solution of a given concentration.

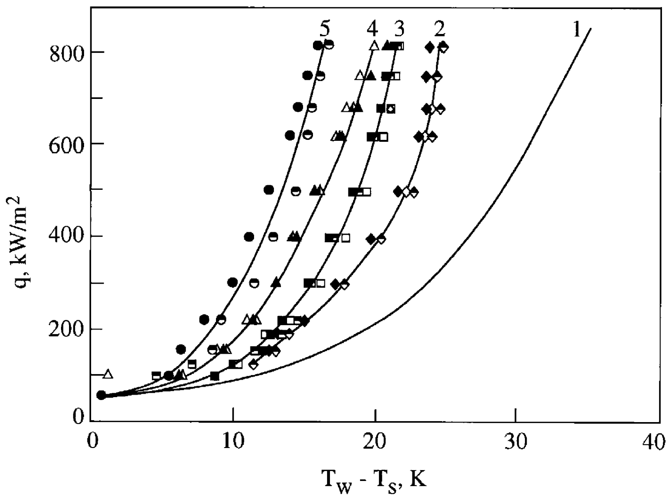

Fig. 8. Subcooled boiling of the fresh Habon G solutions. Symbols are according to the Table 3. The concentration of surfactant C (ppm): 1 – 0 (water), 2 – 130, 3 – 260, 4 – 530, 5 – 1060.

Table 3
Symbols

C (ppm)	T_B (°C)		
	40	60	70
130	◇	⬘	◆
260	□	⬒	■
530	△	◭	▲
1060	○	◓	●
0	▽	⧨	▼

Visual observations showed that the presence of Habon G additive in water produced a large number of small diameter bubbles, which, at high heat fluxes, tended to cover the entire heater surface, causing an increase in the heater wall temperature. Bubbles from a given nucleation site have a distribution of sizes, and frequencies depending on the solution concentration, bulk temperature and heat flux.

The role of surface tension as one of the primary determinants of the boiling behavior has long be considered in the literature (see e.g. Westwater, 1956). In the studies on pool boiling of surfactants the equilibrium surface tension was measured at room temperature (Wasekar and Manglik, 2000; Yang and Maa, 2001). The surface tension changes significantly with increase in the solution temperature. For example, the surface tension of the 530 ppm Habon G solution decreases more than twice in the temperature range of 25–70 °C (Fig. 1). On the other hand, these changes do not affect the behavior of boiling curve.

Besides the surface tension other thermo-physical properties of surfactant may be affected by the additive. Such properties as density and heat capacity were essentially taken to be those of the solvent, since the concentration did not exceed 1060 ppm. Our measurements have shown that thermal conductivity of the solution was not altered with the concentration. It can be seen also (Fig. 8), that kinematic viscosity, at given concentration, did not affect significantly the heat transfer, in spite of an decrease in its magnitude with an increase in the temperature.

Fig. 8 indicates great enhancement of heat transfer with increasing the concentration of the solution. One of the reasons for such a behavior may be related to the diffusion-controlled mechanisms for ionic surfactants proposed by Henneberg et al. (1980). They supposed that diffusion of surfactant molecules and their adsorption rates govern the number of active nucleation sites.

4.3. Degraded solutions

Above, the attention was focused on the boiling heat transfer in fresh solution of Habon G. We now discuss the results related to heat transfer in degraded surfactant solutions, i.e. solutions which undergo repeated heating and cooling.

The following procedure was employed to test the effect of heating on the macroscopical properties of surfactant solution. After a number of runs of a stable boiling a small amount of the fluid sample was taken for measurement of the viscosity. After that the heating power was increased and the experimental runs started again. It was found that the viscosity of the fresh solution was stable for 1–3 runs, no more, then the viscosity began to change during 4–6 runs (boiling–cooling to ambient temperature) and afterwards did not change again (the relaxation time is about 30–40 h). Such solutions were defined as degraded. We did not observe any change in surface tension and thermal conductivity, compared to the fresh solution.

4.3.1. Visualization of flow pattern

For degraded Habon G solutions, the boiling occurred at wall superheat higher than that observed in fresh solutions and water. The subcooled boiling in both water and fresh Habon G solutions was accompanied by a formation of small bubbles on the heated surface. However, there was observed a significant difference in the behavior of boiling patterns at the onset of boiling in degraded solutions. The boiling incipience in fresh solution is shown in Fig. 9(a). The formation of big vapor cluster takes place in degraded Habon G solution before boiling incipience. The burst of such cluster is shown in Fig. 9(b). The cluster formation was accompanied by high wall superheat in a heat flux-controlled experiments. Finally, the collapse of the cluster leads to reduction in wall superheat and subcooled boiling regime occur.

4.3.2. Boiling hysteresis

The typical results are presented in Fig. 10, where boiling curve of Habon G solutions is depicted. All data in the figure are taken at the bulk solution temperature $T_B = 60$ °C. The onset of boiling corresponds to the curve ABCD for runs with increasing heat flux. It follows the curve DEF for decreasing heat flux. The fluid was kept at subcooled condition for more than an hour before increasing the heat flux. The measurements are repeated several times and the same phe-

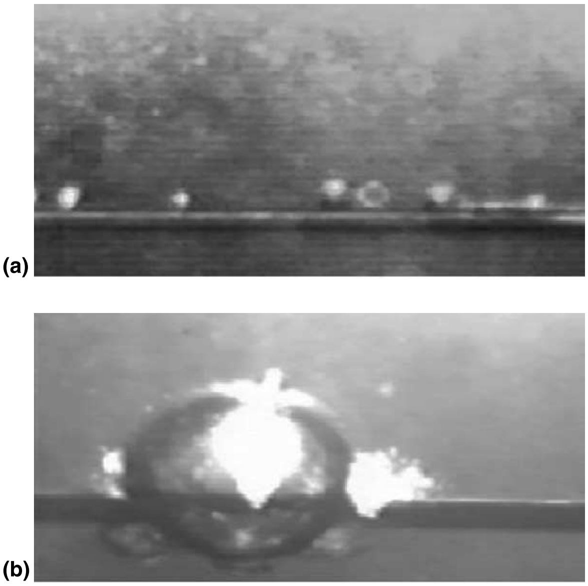

Fig. 9. Incipience of boiling in 530 ppm Habon G solution: (a) fresh solution $q = 260\ \mathrm{kW/m^2}, T_B = 60$ °C, $T_W = 112.3$ °C; (b) degraded solution $q = 260\ \mathrm{kW/m^2}, T_B = 60$ °C, $T_W = 152.4$ °C.

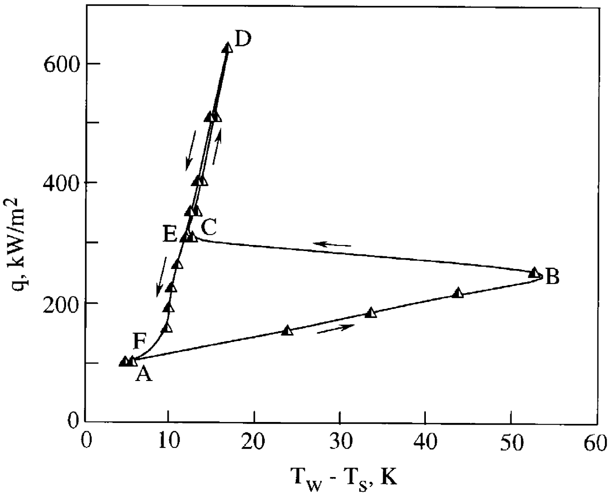

Fig. 10. Subcooled boiling of the degraded Habon G solutions. Bulk temperature $T_B = 60$ °C; $C = 530$ ppm.

nomena are observed. Point B stands for the condition at which the fluid starts to boil when the heat flux is increasing. This point indicates the maximum superheat detected in the test.

It is speculated that molecules of degraded surfactant are more amenable to formation of a surfactant monolayer, which renders the interface less flexible and results in the dampening of interfacial motion. As a consequence, a small amount of surfactant causes a large effect. Further increase in surfactant concentration will produce only small changes in the formation of monolayer. Davies and Wiggill (1960) also reported that surfactant could affect formation of monolayer at the interface.

5. Conclusion

To our knowledge, this is the first study of subcooled boiling of surfactant solution in a pool. The effect on boiling curve of both the concentration of the surfactant solution and the level of subcooling was examined in this study. This consideration was carried out accounting the role of thermal properties of the surfactant solution like surface tension, viscosity and thermal conductivity.

Results of this research become as following:

The boiling curves are quite different from those of clear water for both fresh and degraded solutions.

The boiling curve of the surfactant solution depends on its concentration. Every surfactant solution at given concentration behaves itself as new liquid having the common boiling curve at various level of subcooling.

The increase in the concentration of Habon G enhances the heat transfer considerably.

The present experimental results, and those available in the literature for saturated boiling of surfactants, reveal that neither equilibrium surface tension nor viscosity at a bulk temperature of the solution may be the explanation of the effect surfactant on heat transfer at pool subcooled boiling. This phenomenon may be related to formation of a surfactant monolayer, which results in damping of an interfacial motion.

Boiling hysteresis is found for degraded solutions. The formation of big vapor cluster takes place in degraded Habon G solution before boiling incipience. The cluster formation was accompanied by high wall superheat in a heat flux controlled experiments. Finally, the collapse of the cluster leads to reduction in wall superheat and subcooled boiling regime occur.

Acknowledgements

This research was supported by the Fund for the Promotion of Research at the Technion, M. Gurevich is supported by the Ministry of Absorption, State of Israel, A. Mosyak and R. Rozenblit are supported by a joint grant from the Center for Absorption in Science of the Ministry of Immigrant Absorption and the Committee for Planning and Budgeting of the Council for Higher Education under the framework of the KAMEA program, L.P. Yarin is supported by the Israel council for Higher Education. This research was also supported by Water Research Institute and Rabin Desalination Laboratory.

References

Ammerman, C.N., You, S.M., 1996. Determination of the boiling enhancement mechanism caused by surfactant addition to water. J. Heat Transfer 118, 429–435.

Carey, V.P., 1992. Liquid–Vapor Phase-change Phenomena. Hemisphere, Washington, DC.

Davies, J.T., Wiggill, J.B., 1960. Diffusion across the oil/water interface. Proc. R. Soc. London. Ser. A 255, 277–291.

Gannet Jr., H.J, Williams, M.C., 1971. Pool boiling in dilute non-aqueous solutions. Int. J. Heat Mass Transfer 14, 1001–1005.

Henneberg, M., Sanfeld, A., Bisch, P.M., 1980. Absorption–desorption barrier diffusional exchanges and surface instabilities of longitudinal waves for aperiodic regimes. J. Am. Inst. Chem. Eng. 27, 1002–1008.

Hetsroni, G., Rozenblit, R., 1994. Heat transfer to a liquid–solid mixture in a flume. Int. J. Multiphase Flow 20, 671–689.

Hetsroni, G., Zakin, J.L., Lin, Z., Mosyak, A., Pancallo, E.A., Rozenblit, R., 2001. The effect of surfactants on bubble growth, wall thermal patterns and heat transfer in pool boiling. Int. J. Heat Mass Transfer 44, 485–497.

Hetsroni, G., Zakin, J.L., Mosyak, A., 1997. Low-speed streaks in drag reduced turbulent flow. Phys. Fluids 9, 2397–2404.

Hong, Y.S., Ammerman, C.N., You, S.M., 1997. Boiling characteristics of cylindrical heaters in saturated, gas-saturated, and pure-subcooled FC 72. J. Heat Transfer 119, 313–318.

Johansen, K., 1991. Low quality transition and inverted annular flow film boiling of water: an updated review. Exp. Thermal Fluid Sci. 4, 497–509.

Judd, R.L., Hwang, K.S., 1976. A comprehensive model for nucleate pool boiling heat transfer including microlayer evaporation. J. Heat Transfer 98, 623–629.

Kandlikar, S.G., Alves, L., 1999. Effects of surface tension and binary diffusion on pool boiling of dilute solutions: an experimental assessment. J. Heat Transfer 121, 488–493.

Kline, S.J., McClintock, F.A., 1953. Describing uncertainties in single-sample experiments. Mech. Eng. 75, 3–8.

Morgan, A.I., Bromley, L.A., Wilke, C.R., 1949. Effect of surface tension on heat transfer in boiling. Ind. Eng. Chem. 41, 2767–2771.

Mudawar, I., Anderson, T.M., 1989. High flux electronic cooling by means of pool boiling – Part 1 Parametric investigation of the effects of coolant variation, pressurization, subcooling, and surface augmentation. ASME HTD 111, 25–34.

Sephton, H., 1974. US Patent No. 3846254.

Tzan, Y.L., Yang, Y.M., 1990. Experimental study of surfactant effects on pool boiling heat transfer. J. Heat Transfer 112, 207–212.

Wasekar, V.M., Manglik, R.M., 1999. A review of enhanced heat transfer in nucleate pool boiling of aqueous surfactant and polymeric solutions. Enhanced Heat Transfer 6, 135–150.

Wasekar, V.M., Manglik, R.M., 2000. Pool boiling heat transfer in aqueous solutions of an anionic surfactant. Trans. ASME, J. Heat Transfer 122, 708–715.

Westwater, J.W., 1956. Boiling of liquids. In: Drew, T.B.Hoopes Jr., J.W. (Eds.), Advances in Chemical Engineering, vol. 1. Academic Press, New York.

Wu, W.T., Yang, Y.M., Maa, J.R., 1995. Enhancement of nucleate boiling heat transfer and depression of surface tension by surfactant additives. J. Heat Transfer 117, 526–529.

Yang, Y.M., Maa, J.R, 1983. Pool boiling of dilute surfactant solutions. J. Heat Transfer 105, 190–192.

Yang, Y.M., Maa, J.R., 2001. On the criteria of nucleate pool boiling enhancement by surfactant addition to water. Trans. IchemE79, part A, 409–415.

Zakin, J.L., Myska, J., Chara, Z., 1996. New limiting drag reduction and velocity profile asymptotes for nonpolymeric additives systems. AIChE J. 42, 3544–3546.